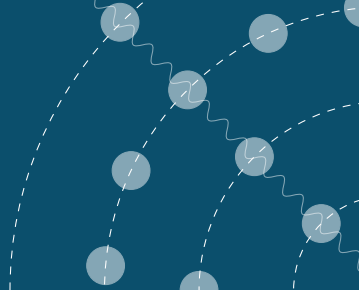
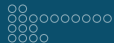
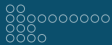


Spectra simulation from first principles for Copper below the ionization threshold using high-performance computing

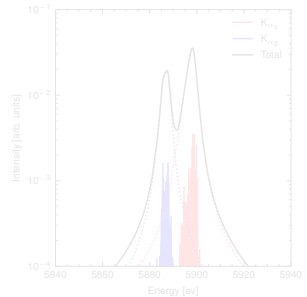
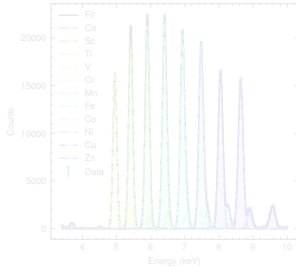
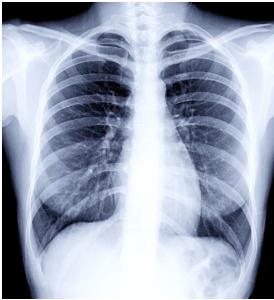




Overview



X-ray applications

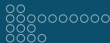


(a) Imaging purposes

(b) Sample quantification

(c) Fundamental parameters

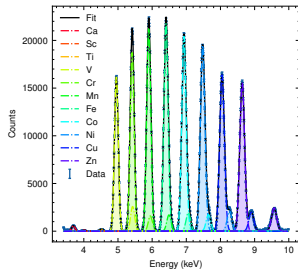
Figure: Application examples of x-ray radiation



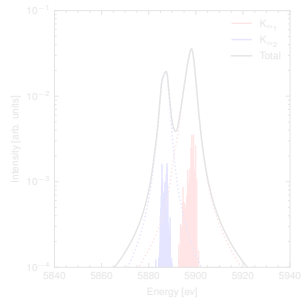
X-ray applications



(a) Imaging purposes

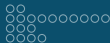


(b) Sample quantification

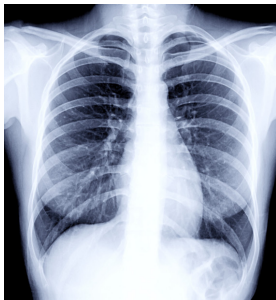


(c) Fundamental parameters

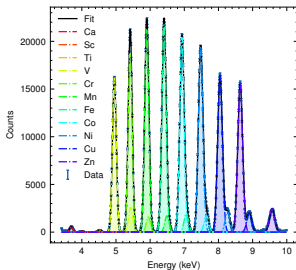
Figure: Application examples of x-ray radiation



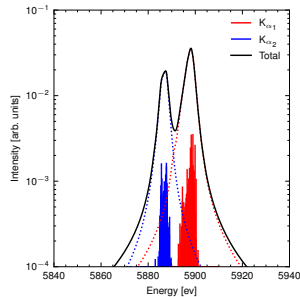
X-ray applications



(a) Imaging purposes

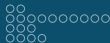


(b) Sample quantification



(c) Fundamental parameters

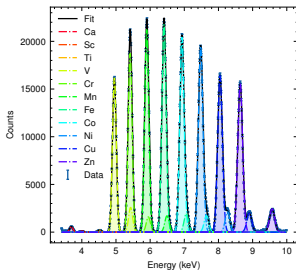
Figure: Application examples of x-ray radiation



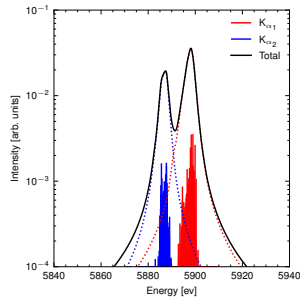
X-ray applications



(a) Imaging purposes



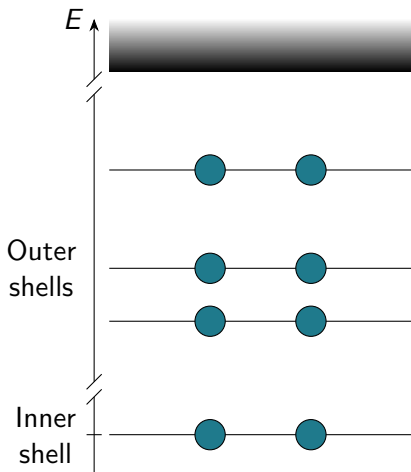
(b) Sample quantification



(c) Fundamental parameters

Figure: Application examples of x-ray radiation

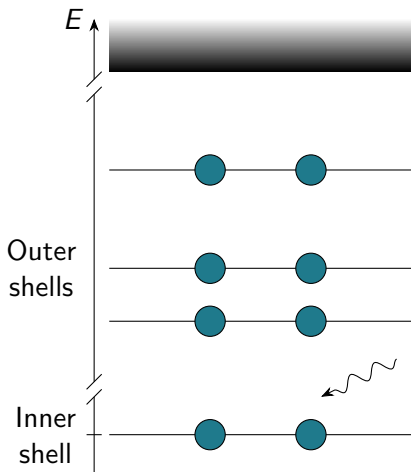
Vacancy generation and relaxation processes



- Bound state system
- Energy transfer
- Ionization
- Vacancy generated
- Atomic Relaxation

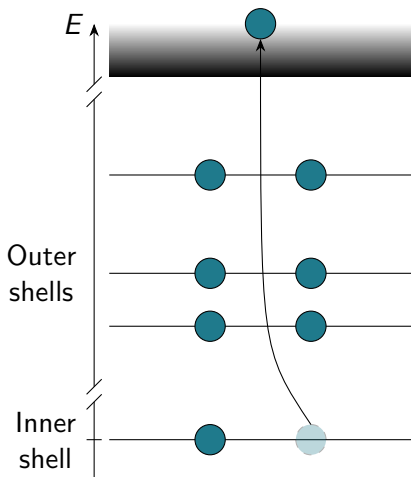


Vacancy generation and relaxation processes

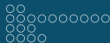


- Bound state system
- Energy transfer
- Ionization
- Vacancy generated
- Atomic Relaxation

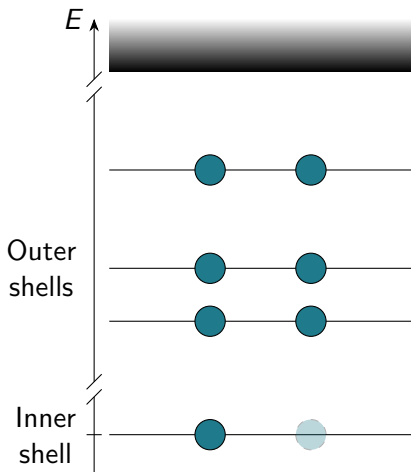
Vacancy generation and relaxation processes



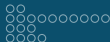
- Bound state system
- Energy transfer
- **Ionization**
- Vacancy generated
- Atomic Relaxation



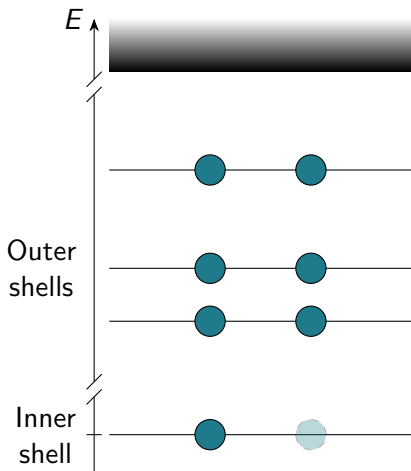
Vacancy generation and relaxation processes



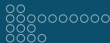
- Bound state system
- Energy transfer
- Ionization
- **Vacancy generated**
- Atomic Relaxation
 - Radiative relaxation (x-ray emission)
 - Auger electron emission



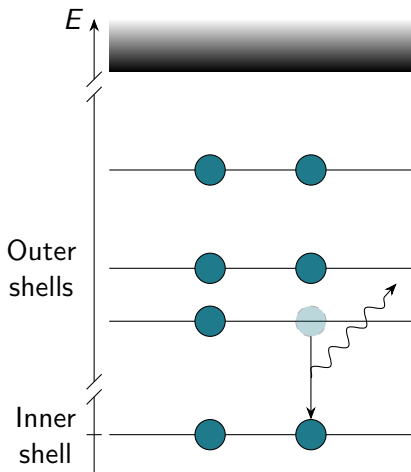
Vacancy generation and relaxation processes



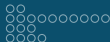
- Bound state system
- Energy transfer
- Ionization
- Vacancy generated
- Atomic Relaxation
 - Radiative relaxation (x-ray emission)
 - Auger electron emission



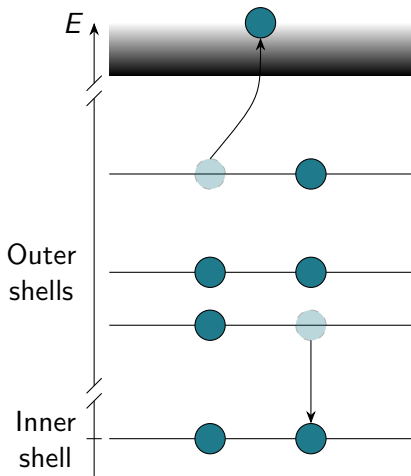
Vacancy generation and relaxation processes



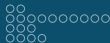
- Bound state system
- Energy transfer
- Ionization
- Vacancy generated
- Atomic Relaxation
 - Radiative relaxation (x-ray emission)
 - Auger electron emission



Vacancy generation and relaxation processes



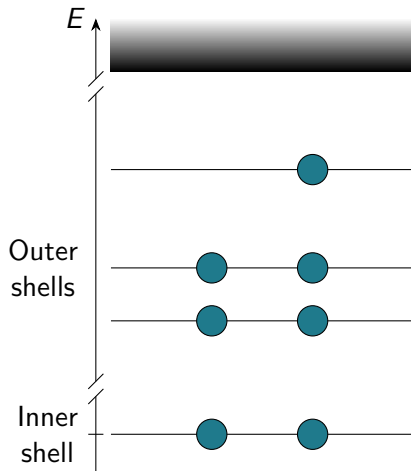
- Bound state system
- Energy transfer
- Ionization
- Vacancy generated
- Atomic Relaxation
 - Radiative relaxation (x-ray emission)
 - Auger electron emission

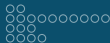


Other processes

Photoexcitation

The most relevant process, for the scope of this work, is that of resonant photoexcitation. In it, instead of a vacancy generated due to sending one electron to the continuum, it has, in turn, remained bound but in a higher energy level.

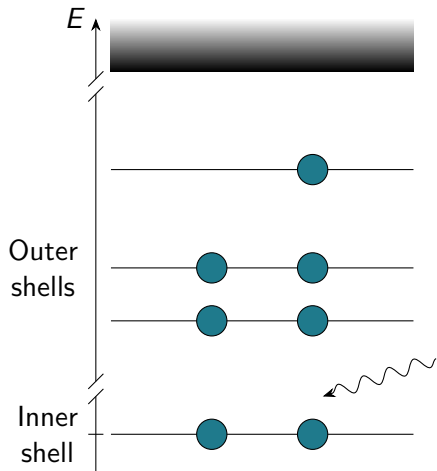


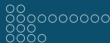


Other processes

Photoexcitation

The most relevant process, for the scope of this work, is that of resonant photoexcitation. In it, instead of a vacancy generated due to sending one electron to the continuum, it has, in turn, remained bound but in a higher energy level.

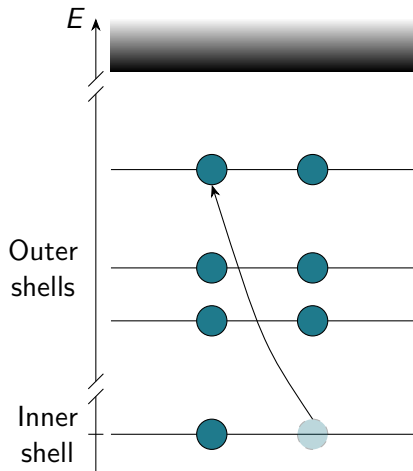




Other processes

Photoexcitation

The most relevant process, for the scope of this work, is that of resonant photoexcitation. In it, instead of a vacancy generated due to sending one electron to the continuum, it has, in turn, remained bound but in a higher energy level.



Schrödinger's Hamiltonian

In its most basic form, for a "classical" atom (nucleus + electrons), and when relativistic effects are not taken into account, the considered Hamiltonian follows the one use in Schrödinger's equation:

$$\hat{H} = \sum_i^N \frac{1}{2} \nabla_i^2 - \frac{Z}{r_i} + \sum_{j>i} + \frac{1}{r_{ij}}$$

It incorporates:

- The kinetic energy of the electron.
- The potential energy of the electron-nucleus attraction.
- The potential energy of the electron-electron repulsion.

Schrödinger's Hamiltonian

In its most basic form, for a "classical" atom (nucleus + electrons), and when relativistic effects are not taken into account, the considered Hamiltonian follows the one use in Schrödinger's equation:

$$\hat{H} = \sum_i^N \frac{1}{2} \nabla_i^2 - \frac{Z}{r_i} + \sum_{j>i} + \frac{1}{r_{ij}}$$

It incorporates:

- The kinetic energy of the electron.
- The potential energy of the electron-nucleus attraction.
- The potential energy of the electron-electron repulsion.

Schrödinger's Hamiltonian

In its most basic form, for a "classical" atom (nucleus + electrons), and when relativistic effects are not taken into account, the considered Hamiltonian follows the one use in Schrödinger's equation:

$$\hat{H} = \sum_i^N \frac{1}{2} \nabla_i^2 - \frac{Z}{r_i} + \sum_{j>i} + \frac{1}{r_{ij}}$$

It incorporates:

- The kinetic energy of the electron.
- The potential energy of the electron-nucleus attraction.
- The potential energy of the electron-electron repulsion.

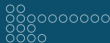
Schrödinger's Hamiltonian

In its most basic form, for a "classical" atom (nucleus + electrons), and when relativistic effects are not taken into account, the considered Hamiltonian follows the one use in Schrödinger's equation:

$$\hat{H} = \sum_i^N \frac{1}{2} \nabla_i^2 - \frac{Z}{r_i} + \sum_{j>i} + \frac{1}{r_{ij}}$$

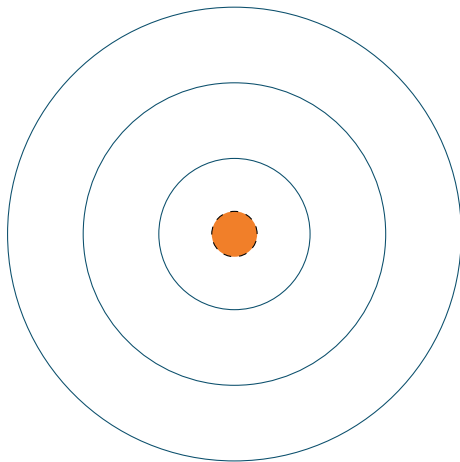
It incorporates:

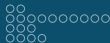
- The kinetic energy of the electron.
- The potential energy of the electron-nucleus attraction.
- The potential energy of the electron-electron repulsion.



Solving the non-relativistic many-body problem

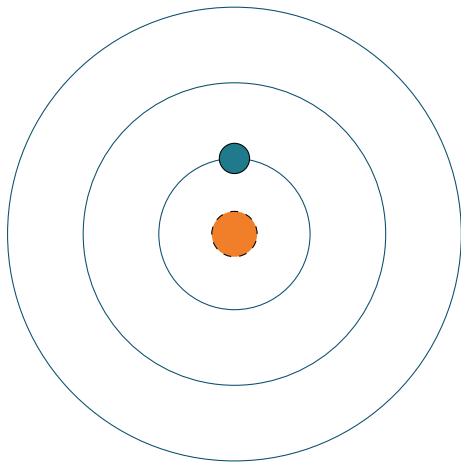
Due to the complexity introduced by the many bodies in the system, and their interactions, a numerical method needs to be employed as to obtain eigenfunctions for this Hamiltonian.





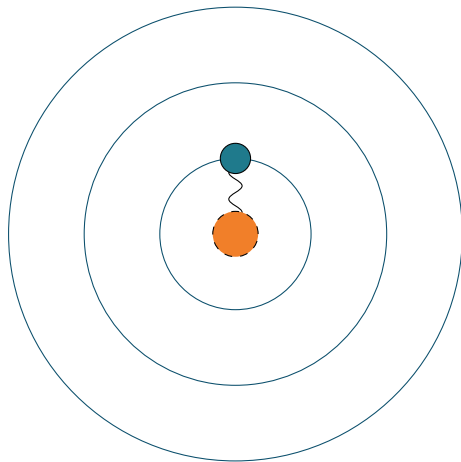
Solving the non-relativistic many-body problem

Due to the complexity introduced by the many bodies in the system, and their interactions, a numerical method needs to be employed as to obtain eigenfunctions for this Hamiltonian.



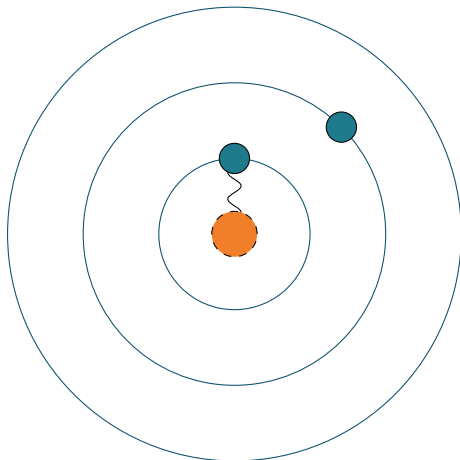
Solving the non-relativistic many-body problem

Due to the complexity introduced by the many bodies in the system, and their interactions, a numerical method needs to be employed as to obtain eigenfunctions for this Hamiltonian.



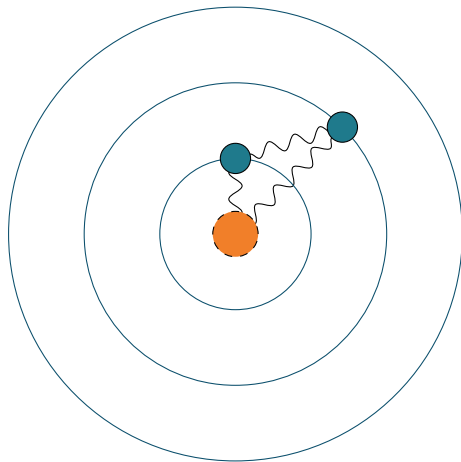
Solving the non-relativistic many-body problem

Due to the complexity introduced by the many bodies in the system, and their interactions, a numerical method needs to be employed as to obtain eigenfunctions for this Hamiltonian.



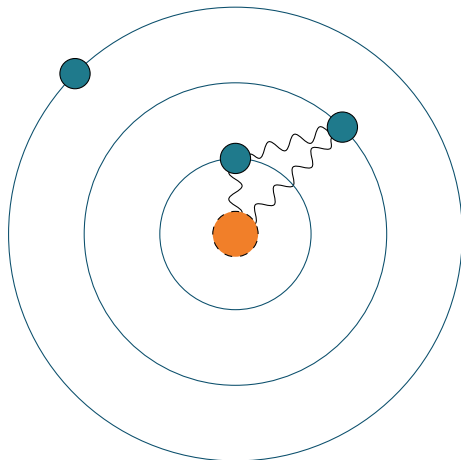
Solving the non-relativistic many-body problem

Due to the complexity introduced by the many bodies in the system, and their interactions, a numerical method needs to be employed as to obtain eigenfunctions for this Hamiltonian.



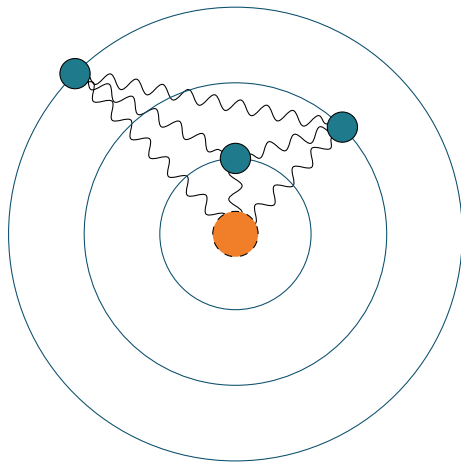
Solving the non-relativistic many-body problem

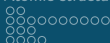
Due to the complexity introduced by the many bodies in the system, and their interactions, a numerical method needs to be employed as to obtain eigenfunctions for this Hamiltonian.



Solving the non-relativistic many-body problem

Due to the complexity introduced by the many bodies in the system, and their interactions, a numerical method needs to be employed as to obtain eigenfunctions for this Hamiltonian.





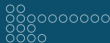
Solving the non-relativistic many-body problem

Each of the electrons' wavefunctions, u , are composed as a product of a spatial part, ψ , and one related to the electron's spin χ .

$$u = \psi\chi$$

The system's wavefunction should then be written as a Slater determinant as to account for anti-symetry and the fermionic nature of the electrons.

$$\frac{1}{\sqrt{N!}} \begin{vmatrix} u_1(x_1) & u_2(x_1) & \dots & u_N(x_1) \\ u_1(x_2) & u_2(x_2) & \dots & u_N(x_2) \\ \vdots & \vdots & \ddots & \vdots \\ u_1(x_N) & u_2(x_N) & \dots & u_N(x_N) \end{vmatrix}$$



Solving the non-relativistic many-body problem

Through a **self-consistent** field approach, the method solves, for each cycle, a set of integro-differential equations as a way to compute new wavefunctions and the new energy for the system.

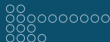
$$E_0 \text{ ————— } N = 0$$

$$E_1 \text{ ————— } N = 1$$

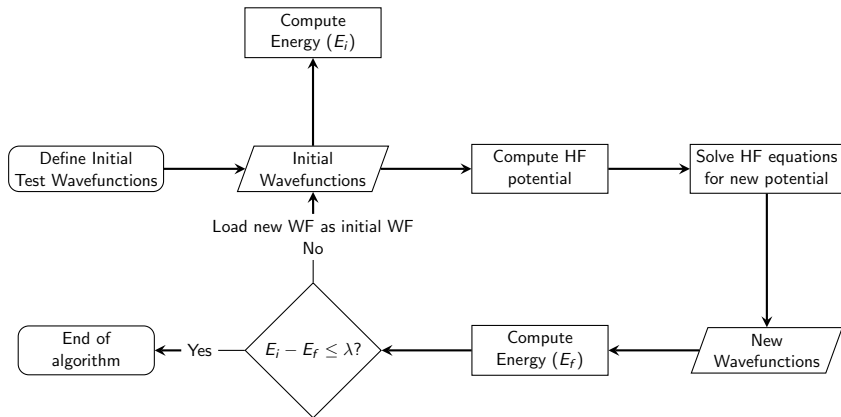
$$E_2 \text{ ————— } N = 2$$

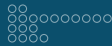
$$E_3 \text{ ————— } N = 3$$

$$E_{\text{opt}} \text{ - - - - - } N = \infty$$



Solving the non-relativistic many-body problem





Limitations of the non-relativistic approach

While Schrödinger's equation may be quite accurate for low energy systems (e.g. Hydrogen), where the speed of the surrounding electrons is not comparable to that of light, such is not the case for more complex and heavier systems.

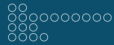
Speed of 1s electrons in ground state configurations (% of c)

Hydrogen: 0.516%

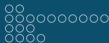
Copper: 14.751%

Uranium: 49.211%

$$E_k = mc^2 \left(\frac{1}{\sqrt{1 - \frac{v^2}{c^2}}} - 1 \right)$$



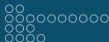
Relativistic approaches



Relativistic approaches

Klein-Gordon equation

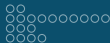
- Incorporates the relativistic energy-mass relation.
- Makes use of relativistic four-vectors.
- Is Lorentz invariant
- Does not account for the effects of the electron spin (valid for $s = 0$).



Relativistic approaches

Klein-Gordon equation

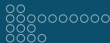
- Incorporates the relativistic energy-mass relation.
- Makes uses of relativistic four-vectors.
- Is Lorentz invariant
- Does not account for the effects of the electron spin (valid for $s = 0$).



Relativistic approaches

Klein-Gordon equation

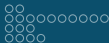
- Incorporates the relativistic energy-mass relation.
- Makes uses of relativistic four-vectors.
- Is Lorentz invariant
- Does not account for the effects of the electron spin (valid for $s = 0$).



Relativistic approaches

Klein-Gordon equation

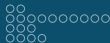
- Incorporates the relativistic energy-mass relation.
- Makes uses of relativistic four-vectors.
- Is Lorentz invariant
- Does not account for the effects of the electron spin (valid for $s = 0$).



Relativistic approaches

Klein-Gordon equation

- Incorporates the relativistic energy-mass relation.
- Makes use of relativistic four-vectors.
- Is Lorentz invariant
- Does not account for the effects of the electron spin (valid for $s = 0$).



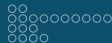
Relativistic approaches

Klein-Gordon equation

- Incorporates the relativistic energy-mass relation.
- Makes uses of relativistic four-vectors.
- Is Lorentz invariant
- Does not account for the effects of the electron spin (valid for $s = 0$).

Dirac equation

- Includes the same advantages as the previous.
- Accounts for spin interactions.
- Yields two-component solutions, for positive and negative energies.
- The "Dirac sea" originated the talks about the possible existence of anti-particles.



Relativistic approaches

Klein-Gordon equation

- Incorporates the relativistic energy-mass relation.
- Makes uses of relativistic four-vectors.
- Is Lorentz invariant
- Does not account for the effects of the electron spin (valid for $s = 0$).

Dirac equation

- Includes the same advantages as the previous.
- Accounts for spin interactions.
- Yields two-component solutions, for positive and negative energies.
- The "Dirac sea" originated the talks about the possible existence of anti-particles.



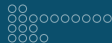
Relativistic approaches

Klein-Gordon equation

- Incorporates the relativistic energy-mass relation.
- Makes uses of relativistic four-vectors.
- Is Lorentz invariant
- Does not account for the effects of the electron spin (valid for $s = 0$).

Dirac equation

- Includes the same advantages as the previous.
- Accounts for spin interactions.
- Yields two-component solutions, for positive and negative energies.
- The "Dirac sea" originated the talks about the possible existence of anti-particles.



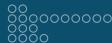
Relativistic approaches

Klein-Gordon equation

- Incorporates the relativistic energy-mass relation.
- Makes uses of relativistic four-vectors.
- Is Lorentz invariant
- Does not account for the effects of the electron spin (valid for $s = 0$).

Dirac equation

- Includes the same advantages as the previous.
- Accounts for spin interactions.
- Yields two-component solutions, for positive and negative energies.
- The "Dirac sea" originated the talks about the possible existence of anti-particles.



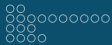
Relativistic approaches

Klein-Gordon equation

- Incorporates the relativistic energy-mass relation.
- Makes uses of relativistic four-vectors.
- Is Lorentz invariant
- Does not account for the effects of the electron spin (valid for $s = 0$).

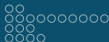
Dirac equation

- Includes the same advantages as the previous.
- Accounts for spin interactions.
- Yields two-component solutions, for positive and negative energies.
- The "Dirac sea" originated the talks about the possible existence of anti-particles.



So, what is missing?

$$H_D = -\frac{e^2 Z}{r} + \beta mc^2 + \alpha \cdot \mathbf{p} \, c.$$



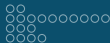
So, what is missing?

$$H_D = -\frac{e^2 Z}{r} + \beta mc^2 + \alpha \cdot \mathbf{p} \, c.$$

Field retardation effects:

Necessary to account for Breit's corrections:

$$H_B = \sum_{i>j} \frac{e^2}{r_{ij}} - e^2 \left(\frac{\alpha_i \alpha_j}{r_{ij}} + \frac{(\alpha_i \nabla_i)(\alpha_j \nabla_j) r_{ij}}{2} \right),$$

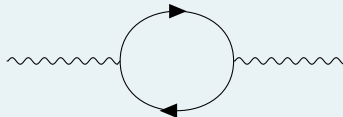


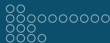
So, what is missing?

$$H = H_D + H_B$$

Field quantization effects (QED):

Necessary to account for effects from Quantum Electrodynamics, such as Self-energy and Vacuum Polarization.



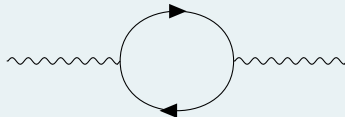


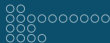
So, what is missing?

$$H = H_D + H_B$$

Field quantization effects (QED):

Necessary to account for effects from Quantum Electrodynamics, such as **Self-energy** and Vacuum Polarization.



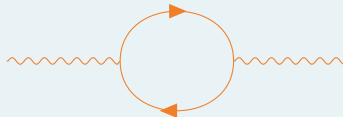


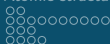
So, what is missing?

$$H = H_D + H_B$$

Field quantization effects (QED):

Necessary to account for effects from Quantum Electrodynamics, such as Self-energy and **Vacuum Polarization**.





The state-of-the-art

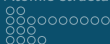
Reasons for this study

- Copper is a dominant element in today's technological progress.
- A great deal of studies has been performed on its emission spectrum.
- Most studies note a skewness in the K_{α} transition lines, being mostly attributed to satellite lines, but leaving open the possibility of its cause coming from **photoexcited states**.
- Few experiments were performed for the near-threshold region, so theory needs to be formed to accompany new experimental data.

The state-of-the-art

Reasons for this study

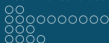
- Copper is a dominant element in today's technological progress.
- A great deal of studies has been performed on its emission spectrum.
- Most studies note a skewness in the K_α transition lines, being mostly attributed to satellite lines, but leaving open the possibility of its cause coming from **photoexcited states**.
- Few experiments were performed for the near-threshold region, so theory needs to be formed to accompany new experimental data.



The state-of-the-art

Reasons for this study

- Copper is a dominant element in today's technological progress.
- A great deal of studies has been performed on its emission spectrum.
- Most studies note a skewness in the K_{α} transition lines, being mostly attributed to satellite lines, but leaving open the possibility of its cause coming from **photoexcited states**.
- Few experiments were performed for the near-threshold region, so theory needs to be formed to accompany new experimental data.



The state-of-the-art

Reasons for this study

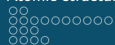
- Copper is a dominant element in today's technological progress.
- A great deal of studies has been performed on its emission spectrum.
- Most studies note a skewness in the K_{α} transition lines, being mostly attributed to satellite lines, but leaving open the possibility of its cause coming from **photoexcited states**.
- Few experiments were performed for the near-threshold region, so theory needs to be formed to accompany new experimental data.

The state-of-the-art

mcdgme (Multi Configuration Dirac-Fock General Matrix Elements)

This code is a novel computational implementation, based on the Hatree-Fock method, capable of calculating a plethora of atomic parameters, while incorporating all previously mentioned necessary considerations.

It has proven time and time again to have excellent accuracy and precision when performing calculations for the most varied systems.



Overview

The considered excitations

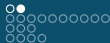
As previously stated, the focal point of this work is that of computing radiative relaxation spectra for excited Copper.

Ground State: $1s^2 2s^2 2p^6 3s^2 3p^6 3d^{10} 4s^1$



Excitations of any one of the constituent electrons to orbitals:

$4s$	$4p$	$4d$	$4f$		
$5s$	$5p$	$5d$	$5f$	$5g$	
$6s$	$6p$	$6d$	$6f$	$6g$	$6h$
$7p$	$8p$	$9p$			



The calculated configurations

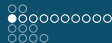
In order to account to all possible decay possibilities, it was necessary to perform calculations for two different sets of configurations.

1-hole configurations

Related to the initial and final states of radiative transitions. Obtained by running a hole through all orbitals in the base-configurations.

2-holes configurations

Related to the final states of Auger transitions. Obtained by running a combination of two holes through all orbitals in the base-configurations.



The level manifold

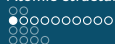
It is now necessary to compute all possible levels the studied atomic system can be in. As it will be shown, this is no simple task. . .



The level manifold

Besides the original configuration, three other sets of quantum numbers are necessary for defining a level:

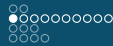
- The hole orbital labels ($n l_j$)
- The total angular momentum number J
- The eigenvalue/Lagrange multiplier ϵ



The level manifold

Besides the original configuration, three other sets of quantum numbers are necessary for defining a level:

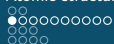
- The hole orbital labels ($n l_j$)
- The total angular momentum number J
- The eigenvalue/Lagrange multiplier ϵ



The level manifold

Besides the original configuration, three other sets of quantum numbers are necessary for defining a level:

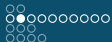
- The hole orbital labels ($n l_j$)
- The total angular momentum number J
- The eigenvalue/Lagrange multiplier ϵ



The level manifold

Besides the original configuration, three other sets of quantum numbers are necessary for defining a level:

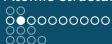
- The hole orbital labels ($n l_j$)
- The total angular momentum number J
- The eigenvalue/Lagrange multiplier ϵ



The level manifold- an example: $4p$ excited Copper

Here, we know two base things:

- The ground state configuration.
- One of the electrons was excited to $4p$



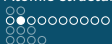
The level manifold- an example: $4p$ excited Copper

Here, we know two base things:

- The ground state configuration.
- One of the electrons was excited to $4p$

This leads to the possibility of the electron having come from:

- $1s$
- $2s$
- $2p$
- $3s$
- $3p$
- $3d$
- $4s$



The level manifold- an example: $4p$ excited Copper

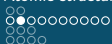
Here, we know two base things:

- The ground state configuration.
- One of the electrons was excited to $4p$

These are the **labels** ($n l_j$). 7 in total.

This leads to the possibility of the electron having come from:

- $1s$
- $2s$
- $2p$
- $3s$
- $3p$
- $3d$
- $4s$



The level manifold- an example: $4p$ excited Copper

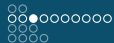
Here, we know two base things:

- The ground state configuration.
- One of the electrons was excited to $4p$

These are the **labels** ($n l_j$). 7 in total.
Let us analyse an excitation from $2p$.

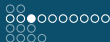
This leads to the possibility of the electron having come from:

- $1s$
- $2s$
- $2p$
- $3s$
- $3p$
- $3d$
- $4s$



The level manifold- an example: $2p \rightarrow 4p$ excited Copper

For this configuration, three subshells are open: $2p$, $4s$, and $4p$.



The level manifold- an example: $2p \rightarrow 4p$ excited Copper

For this configuration, three subshells are open: $2p$, $4s$, and $4p$.

The different angular momentum couplings lead to various values for system's total angular momentum.

The level manifold- an example: $2p \rightarrow 4p$ excited Copper

For this configuration, three subshells are open: $2p$, $4s$, and $4p$.

The different angular momentum couplings lead to various values for **system's total angular momentum**.

Possibilities for J values follow:

2p		4s		4p		Total/ J
M_l	M_s	M_l	M_s	M_l	M_s	$M_l + M_s$
1	$-1/2$	0	$-1/2$	1	$-1/2$	$1/2$
1	$1/2$	0	$-1/2$	1	$-1/2$	$3/2$
1	$1/2$	0	$1/2$	1	$-1/2$	$5/2$
1	$1/2$	0	$1/2$	1	$1/2$	$7/2$

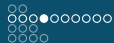
The level manifold- an example: $2p \rightarrow 4p$ excited Copper

For this configuration, three subshells are open: $2p$, $4s$, and $4p$.

The different angular momentum couplings lead to various values for **system's total angular momentum**.

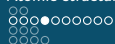
Possibilities for J values follow:

2p		4s		4p		Total/ J
M_l	M_s	M_l	M_s	M_l	M_s	$M_l + M_s$
1	$-1/2$	0	$-1/2$	1	$-1/2$	$1/2$
1	$1/2$	0	$-1/2$	1	$-1/2$	$3/2$
1	$1/2$	0	$1/2$	1	$-1/2$	$5/2$
1	$1/2$	0	$1/2$	1	$1/2$	$7/2$



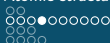
The level manifold- an example: $2p \rightarrow 4p, J = 5/2$

Even for this **very** specific example, the branching-out continues:



The level manifold- an example: $2p \rightarrow 4p, J = 5/2$

There are many possibilities for achieving this certain combination of a given configuration and J value. Each, is represented by the respective ϵ .



The level manifold- an example: $2p \rightarrow 4p$, $J = 5/2$

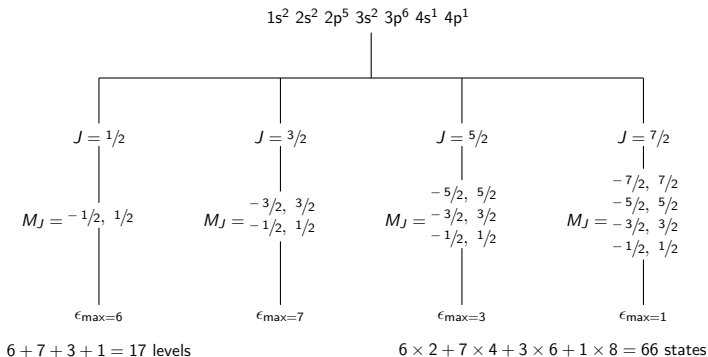
There are many possibilities for achieving this certain combination of a given configuration and J value. Each, is represented by the respective ϵ .

$J = 5/2$					
2p		4s		4p	
M_l	M_s	M_l	M_s	M_l	M_s
1	$-1/2$	0	$1/2$	1	$1/2$
1	$1/2$	0	$-1/2$	1	$1/2$
1	$1/2$	0	$1/2$	1	$-1/2$



The level manifold

This set of possibilities and rearrangements form what we call **the level manifold**. In addition, a $2J + 1$ level degeneracy is accounted for.



Level calculations with *mcdfgme*

A calculation was performed for each existent level.

In each of them, a level was treated as a linear combination of state wavefunctions (associated with the eigenvalues) with mixing coefficients:

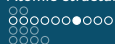
$$|\Psi\rangle = a_1 |\psi_1\rangle + a_2 |\psi_2\rangle + \dots$$

Self-consistent field

- Coulomb interactions
- Breit considerations
- Vacuum Polarization

Perturbation theory

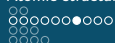
Self-energy



Evaluating the calculation

What to look out for:

- Orthogonality conservation
- Energy divergences
- Effective nuclear charge



Evaluating the calculation

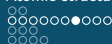
What to look out for:

- Orthogonality conservation
- Energy divergences
- Effective nuclear charge

Due to the method's numerical nature, orthogonality problems may surge.

We look at overlap values for similar orbitals (same l_j) and set a maximum threshold:

$$|\langle n l_j | m l_j \rangle| \leq 10^{-6}$$



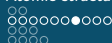
Evaluating the calculation

What to look out for:

- Orthogonality conservation
- Energy divergences
- Effective nuclear charge

A component of the energy is computed through two different methods. For good convergence, the difference in their values should not be above 1 eV.

$$|E_1 - E_2| \leq 1 \text{ eV}$$

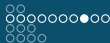


Evaluating the calculation

What to look out for:

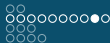
- Orthogonality conservation
- Energy divergences
- **Effective nuclear charge**

The presence of inner electrons leads to a shielding of the positive nuclear charge. As so, outer electrons will be subject to an attenuated positive charge. This effect has been previously studied, and the obtained values should be benchmarked.

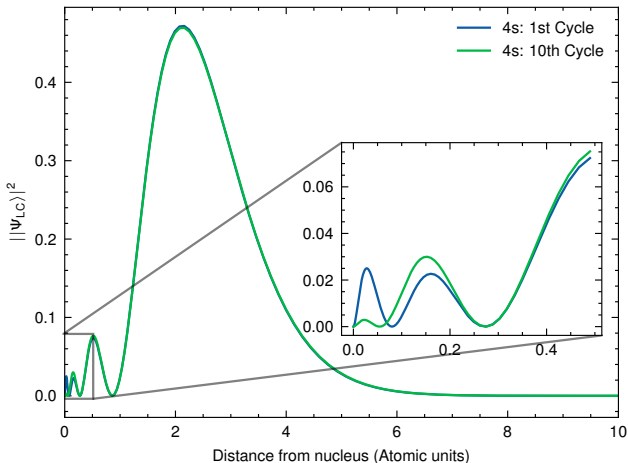


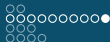
Methods for solving the convergence problems

- Changing the parameters of the self-consistent cycle.
- Choosing the initial trial wavefunctions for select orbitals (e.g. Hydrogenoids or obtained through the Thomas Fermi potential).
- Using other methods for solving the Dirac equation.
- Enforcing the node number for the wavefunctions



Changes in wavefunctions after the variational process





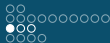
Total number of calculated levels

For the 19 performed calculations,

- 1601 1-hole levels
 - 166 manually converged
- 20550 2-holes levels
 - 1678 manually converged

Leaving a total of:

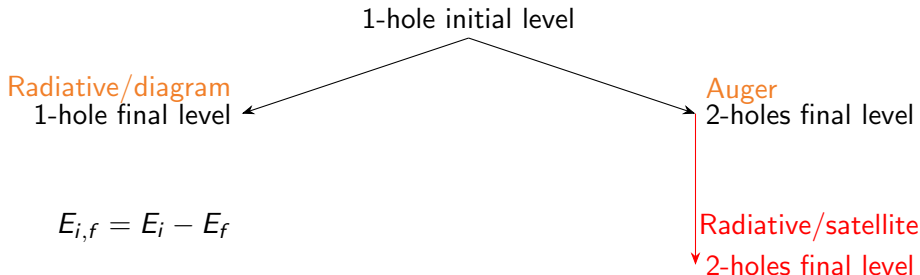
- 22151 levels calculated
- 1844 levels manually converged



Atomic transitions

When a system is not found in its least energetic state various processes will occur until the most stable one is reached.

In this way, for every level, calculations were performed for decays to all possible lower energy states.





All calculated transitions

The total number of transitions calculated:

- 70885 radiative diagram
- 452988 Auger
- 6684258 radiative satellite



All calculated transitions

The total number of transitions calculated:

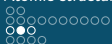
- 70885 radiative diagram
- 452988 Auger
- 6684258 radiative satellite



All calculated transitions

The total number of transitions calculated:

- 70885 radiative diagram
- 452988 Auger
- 6684258 radiative satellite



All calculated transitions

The total number of transitions calculated:

- 70885 radiative diagram
- 452988 Auger
- 6684258 radiative satellite

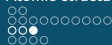


All calculated transitions

The total number of transitions calculated:

- 70885 radiative diagram
- 452988 Auger
- 6684258 radiative satellite

Totaling to 7208131 computations performed.

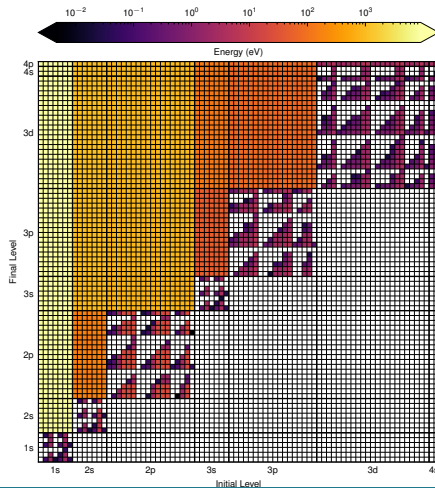
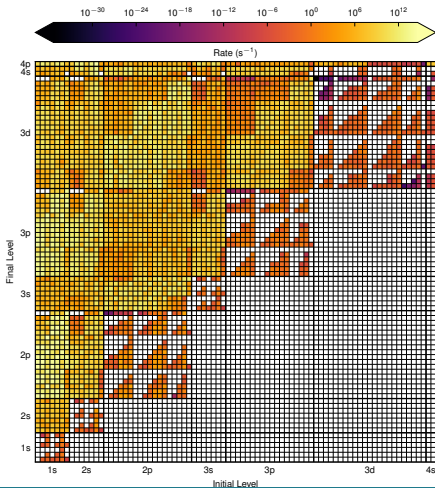


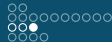
Rate and Energy matrices

To evaluate and benchmark a calculation, a visualization tool was used, where the calculated **energy** and **rate** values were displayed in a grid-like view.

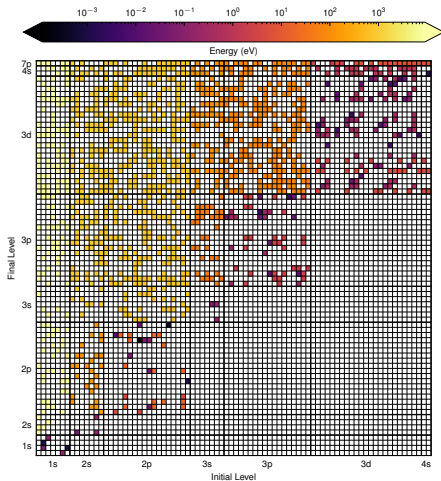
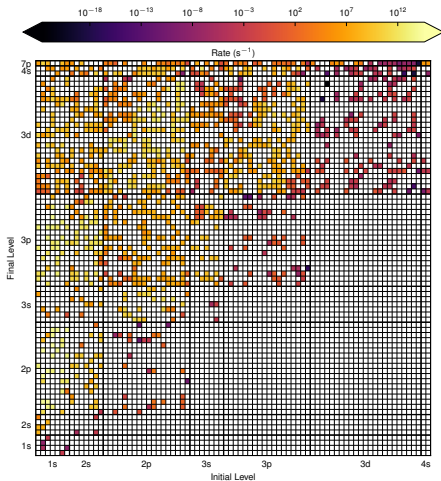


Rate and Energy matrices





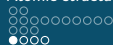
Rate and Energy matrices





Total radiative and non-radiative rates

After computing all possible transitions, one can now start to evaluate certain atomic parameters.



Total radiative and non-radiative rates

To start, the total radiative and non-radiative rates for each level should be computed. When compared, they can provide information on the probability of said level decaying either way.

$$R_i^R = (2J_i + 1) \sum_f R_{i,f}^R$$

$$R_i^{NR} = (2J_i + 1) \sum_f R_{i,f}^{NR}$$



Fluorescence Yield

The quantity is an indicator of the probability of a level decaying either via the emission of a photon as opposed to an Auger electron.

It is given by the ratio between the level's radiative and total rates:

$$\omega_i = \frac{R_i^R}{R_i^R + R_i^{NR}}$$



Fluorescence Yield

For ionized Copper, the K shell F.Y. was computed to be 45.34%.

Every calculated excited state presented a value inferior to this.

Minimum value:

6s-excited Copper

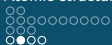
18.09%

Maximum value:

4s-excited Copper

44.88%

This decrease can be explained by the presence of an extra electron increasing the number of Auger channels.



Fluorescence Yield

Other subshells

For other subshells, save for $M_{4,5}$, the F.Y. slightly oscillated around the obtained value for ionized Copper, but mostly **preserving the same order of magnitude**.

$M_{4,5}$ subshells

Curiously both for ionized Copper and for all excitations to ns orbitals, as well as $4p$ and $5p$, **only radiative decays occur**, while for the rest, **Auger transitions reign**.



Level widths

Quantum mechanics tells us bound systems are arranged in states with **quantized energy**, hence why a discrete amount of levels was calculated, a not a continuum.



Level widths

It does, however, also alert us to natural uncertainties, as described by the well-known **Heisenberg uncertainty principle**.



Level widths

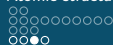
While the momentum-position relation is certainly the most famous one, its energy-time counterpart will have implications in the next steps:



Level widths

While the momentum-position relation is certainly the most famous one, its energy-time counterpart will have implications in the next steps:

$$\Delta E \Delta t \geq \hbar$$



Level widths

$$\Delta E \Delta t \geq \hbar$$

From this, we can naturally deduce that, a level which decays to other lower energy ones ($R \rightarrow \frac{1}{\Delta t}$), should, in principle, also have an **energy width**.

As such, we define the level width as:

$$\Gamma_i = \hbar \cdot (R_i^R + R_i^{NR})$$



Level widths

$$\Delta E \Delta t \geq \hbar$$

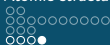
From this, we can naturally deduce that, a level which decays to other lower energy ones ($R \rightarrow \frac{1}{\Delta t}$), should, in principle, also have an **energy width**.

As such, we define the level width as:

$$\Gamma_i = \hbar \cdot (R_i^R + R_i^{NR})$$

And the width of a transition as the sum of the widths for the initial and final level:

$$\Gamma_{i,f} = \Gamma_i + \Gamma_f$$



Transition intensities

Now that many atomic parameters are calculated, it is possible to calculate the spectral intensity of a given transition.

$$I_{i,f} = N_i \frac{2J_i + 1}{g_{\text{sub}}} \frac{R_{i,f}}{R_i^R + R_i^{NR}}$$

Put into simple terms, the intensity is nothing more than the product of the statistical weight of the level multiplicity, of the individual rate compared to the total one, and a scaling factor accounting for population generation.

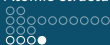


Transition intensities

Now that many atomic parameters are calculated, it is possible to calculate the spectral intensity of a given transition.

$$I_{i,f} = N_i \frac{2J_i + 1}{g_{\text{sub}}} \frac{R_{i,f}}{R_i^R + R_i^{NR}}$$

Put into simple terms, the intensity is nothing more than the product of the statistical weight of the **level multiplicity**, of the individual rate compared to the total one, and a scaling factor accounting for population generation.

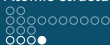


Transition intensities

Now that many atomic parameters are calculated, it is possible to calculate the spectral intensity of a given transition.

$$I_{i,f} = N_i \frac{2J_i + 1}{g_{\text{sub}}} \frac{R_{i,f}}{R_i^R + R_i^{NR}}$$

Put into simple terms, the intensity is nothing more than the product of the statistical weight of the level multiplicity, of the **individual rate** compared to the total one, and a scaling factor accounting for population generation.

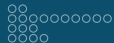


Transition intensities

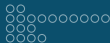
Now that many atomic parameters are calculated, it is possible to calculate the spectral intensity of a given transition.

$$I_{i,f} = N_i \frac{2J_i + 1}{g_{\text{sub}}} \frac{R_{i,f}}{R_i^R + R_i^{NR}}$$

Put into simple terms, the intensity is nothing more than the product of the statistical weight of the level multiplicity, of the individual rate compared to the total one, and a **scaling factor accounting for population generation**.



Overview



The theoretical spectral shape

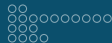
Based on all previously computed atomic parameters, it is now possible to start simulating spectral lines.

Lorentzian profile

Describes the theoretical line shape for the emission:

$$\frac{I_{i,f}}{2\pi} \frac{\Gamma_{i,f}}{(E - E_{i,f})^2 + (\Gamma_{i,f}/2)^2}$$

Does not account for **thermal distributions** and **stochastic events**.

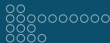


The incident beam

For the purpose of this work, the desired source of radiation for such study would be a synchrotron line.

- Due to the usage of wigglers and undulators, the beam can be close to monochromatic.
- The energy of the radiation used is tunable, allowing for the survey from regions below to post-ionization threshold.

As such, a beam profile of 0.5 eV was considered.



What about N_i ? The photoexcitation effect

The computation of this parameter is somewhat tricky.

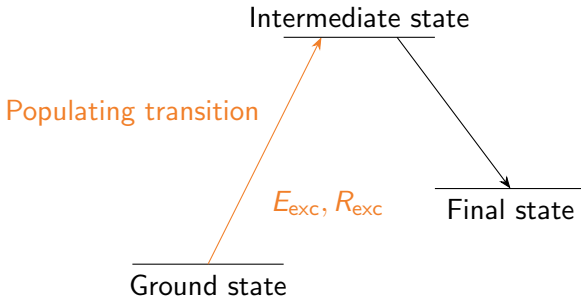
- No analytical expression for cross-sections could be found.
- Should be calculated ab-initio (no data from outside).
- Must simulate the resonance effect.
- Needs to be valid (according to the laws of physics).
- The beam profile should be considered.

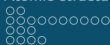
What about N_i ? The photoexcitation effect

The proposed solution:

To solve this problem, an *ad-hoc* expression was developed.

The **rate** and **energy** of the transition from ground state to the excited state was considered by looking at the inverse transition.

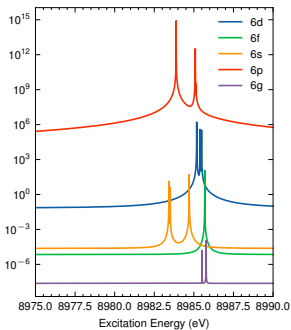
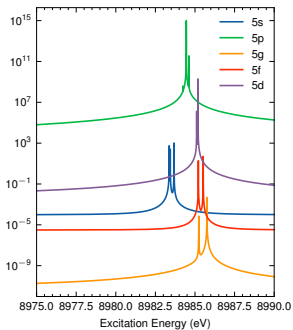
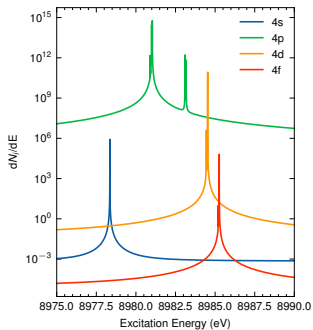


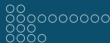


What about N_i ? The photoexcitation effect

A Lorentzian profile was then created using both the energy value, and the associated rate. The overlap between this profile and the beam's was computed and normalized to the rate:

$$N_i = R_{\text{exc}} \int_{-\infty}^{\infty} G(E - E_{\text{beam}}, 0.5 \text{ eV}) \cdot L(E - E_{\text{exc}}, \Gamma_{\text{exc}}) \, dE$$





What about N_i ? The photoionization effect

For energies over the threshold, ionization starts to occur. This effect, will be the predominant one, once the threshold is reached.

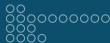
For K-shell ionization, there are **two possible levels**, with different values of total angular momentum:

$$J = 0$$

- 1s, 4s counteraligned spins.
- Multiplicity of 1
- Edge energy of 8986.02 eV

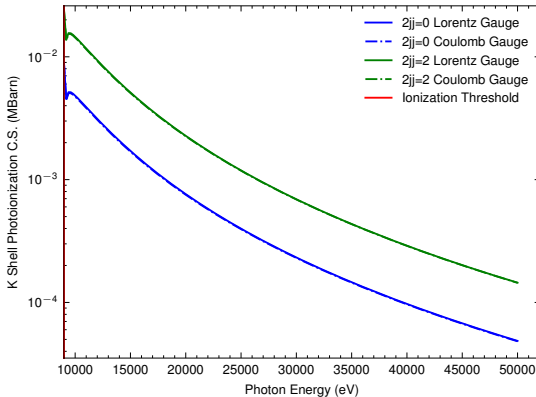
$$J = 1$$

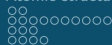
- 1s, 4s aligned spins.
- Multiplicity of 3
- Edge energy of 8985.93 eV



What about N_i ? The photoionization effect

The differential oscillator strength were calculated by performing *mcdfigme* calculations for different incoming photon energies:

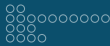




What about N_i ? The photoionization effect

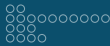
Oscillator strength \leftrightarrow Rate

$$O_s = 2.304 \cdot 10^{-8} [\text{eV}^2\text{s}] \cdot \frac{g_{fin}/g_{in}}{E^2} \cdot R$$



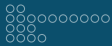
What about N_i ? The photoionization effect

In a similar fashion, N_i was computed by the overlap between these profiles and the beam's.



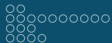
Compiling the results

After this extremely extensive process, it is now finally possible to account for every interaction, and build a synthetic spectrum.



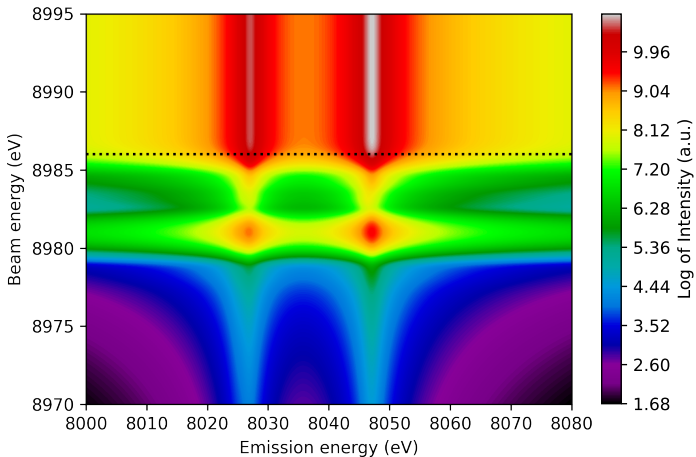
Compiling the results

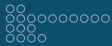
By accounting for every one of the thousands of computed transitions we get...



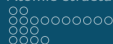
The synthetic spectrum

The final spectrum



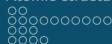


Overview



The analysis profiles

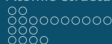
As previously stated, each spectral line is, in reality composed by a great set of many others. As such, it is not expected to be symmetric, and single Lorentzian and Gaussian profiles are not suited for spectral analysis.



The analysis profiles

For each spectral line (K_{α_1} or K_{α_2}), an asymmetric Lorentzian profile was fitted, and an analysis was performed throughout the beam energies.

$$\frac{I}{2\pi} \frac{\Gamma}{\left(\frac{E-E_x}{\alpha \cdot \text{sign}(E-E_x)+1} \right)^2 + (\Gamma/2)^2}$$

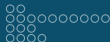


The analysis profiles

For each spectral line (K_{α_1} or K_{α_2}), an asymmetric Lorentzian profile was fitted, and an analysis was performed throughout the beam energies.

$$\frac{I}{2\pi} \frac{\Gamma}{\left(\frac{E-E_x}{\alpha \cdot \text{sign}(E-E_x)+1} \right)^2 + (\Gamma/2)^2}$$

Aside from the Intensity, the Energy, and the Width parameters, it also now includes an asymmetry index.

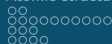


The analysis profiles

For each spectral line (K_{α_1} or K_{α_2}), an asymmetric Lorentzian profile was fitted, and an analysis was performed throughout the beam energies.

$$\frac{I}{2\pi} \frac{\Gamma}{\left(\frac{E-E_x}{\alpha \cdot \text{sign}(E-E_x)+1} \right)^2 + (\Gamma/2)^2}$$

Aside from the **Intensity**, the Energy, and the Width parameters, it also now includes an asymmetry index.

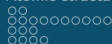


The analysis profiles

For each spectral line (K_{α_1} or K_{α_2}), an asymmetric Lorentzian profile was fitted, and an analysis was performed throughout the beam energies.

$$\frac{I}{2\pi} \frac{\Gamma}{\left(\frac{E - E_x}{\alpha \cdot \text{sign}(E - E_x) + 1} \right)^2 + (\Gamma/2)^2}$$

Aside from the Intensity, the **Energy**, and the Width parameters, it also now includes an asymmetry index.

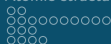


The analysis profiles

For each spectral line (K_{α_1} or K_{α_2}), an asymmetric Lorentzian profile was fitted, and an analysis was performed throughout the beam energies.

$$\frac{I}{2\pi} \frac{\Gamma}{\left(\frac{E-E_x}{\alpha \cdot \text{sign}(E-E_x)+1} \right)^2 + (\Gamma/2)^2}$$

Aside from the Intensity, the Energy, and the Width parameters, it also now includes an asymmetry index.

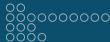


The analysis profiles

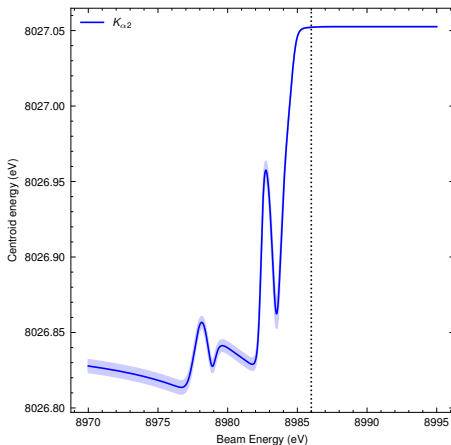
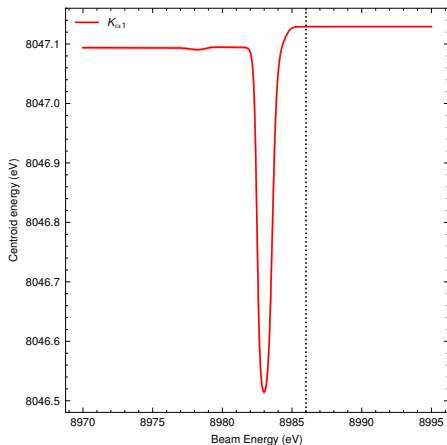
For each spectral line (K_{α_1} or K_{α_2}), an asymmetric Lorentzian profile was fitted, and an analysis was performed throughout the beam energies.

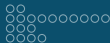
$$\frac{I}{2\pi} \frac{\Gamma}{\left(\frac{E-E_x}{\alpha \cdot \text{sign}(E-E_x)+1} \right)^2 + (\Gamma/2)^2}$$

Aside from the Intensity, the Energy, and the Width parameters, it also now includes an **asymmetry index**.

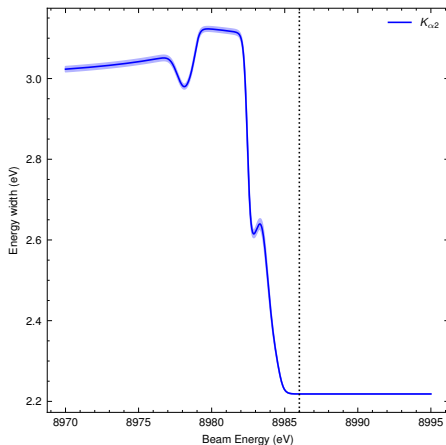
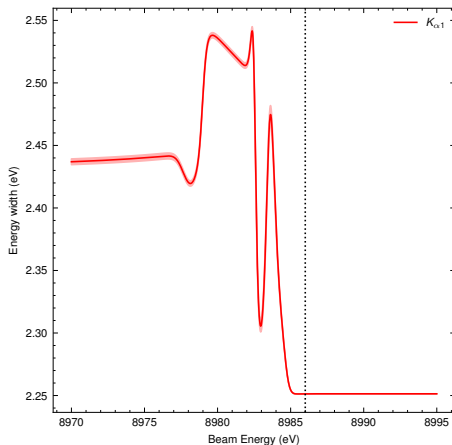


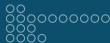
Transition energy



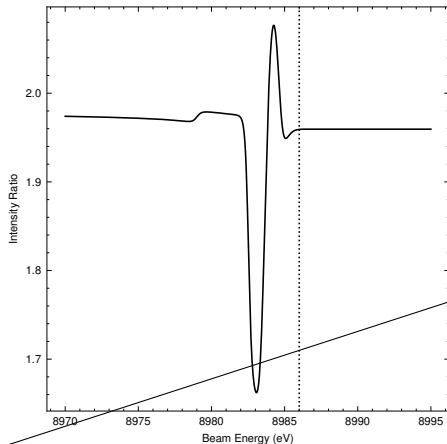
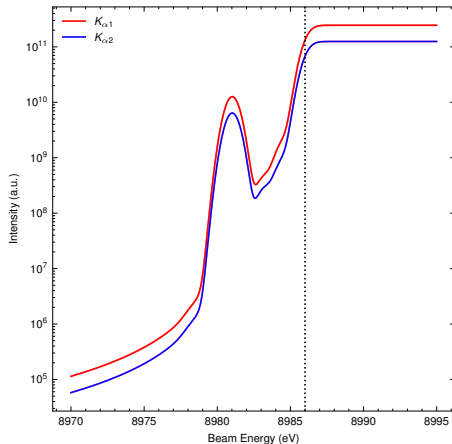


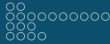
Transition width



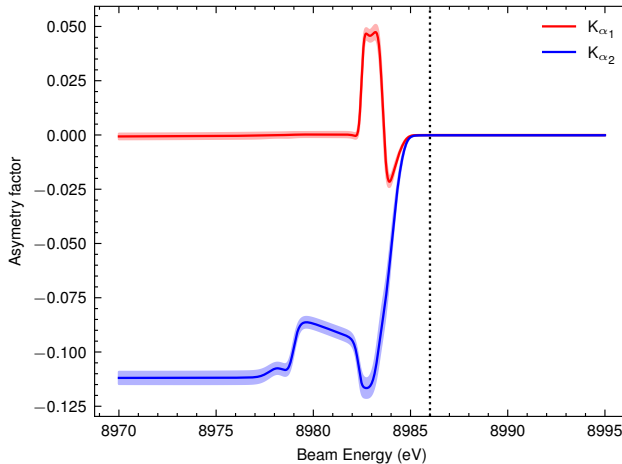


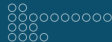
Spectral intensity



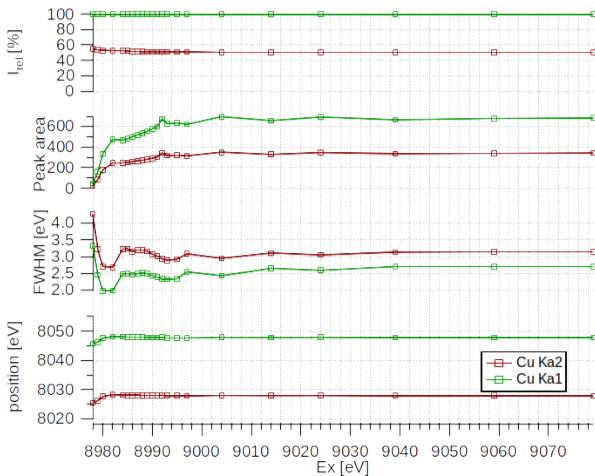


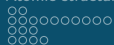
Asymmetry index



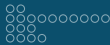


Experimental spectrum from a synchrotron line





Overview



Why the necessity?

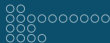
As previously stated, the amount of calculations needed to be performed makes manual calculations simply unfeasible.



Why the necessity?

But is a simple automation algorithm enough?

No, even with a conventional implementation of an automation script, the amount of time needed for the computation would still be unreasonable.

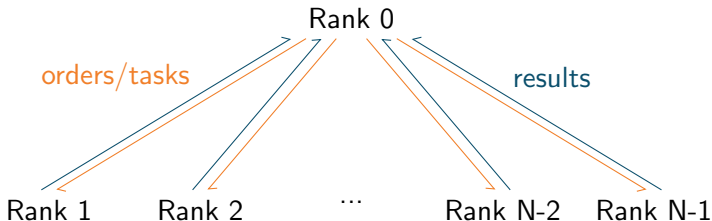


Why the necessity?

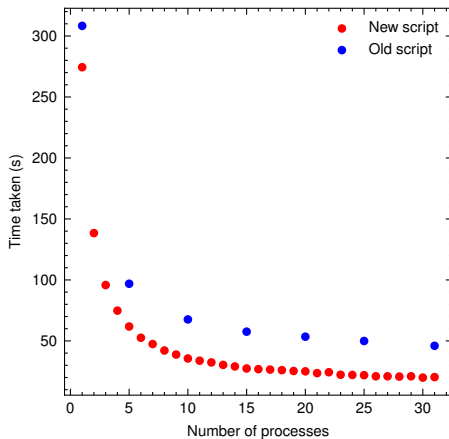
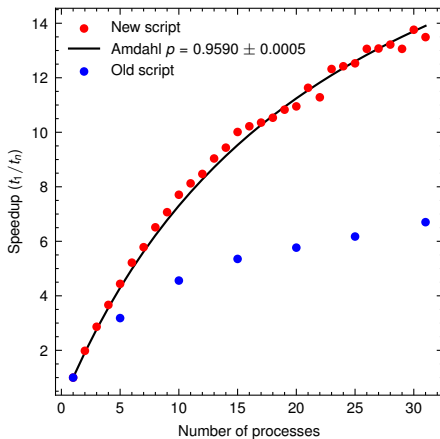
The solution? Parallelization.

A *master-rank* implementation was used in order to tackle this challenge.

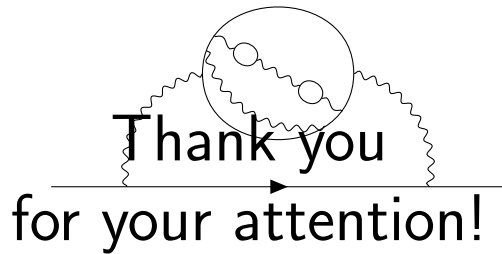
- Using Python due to its flexibility
- Using MPI due to its scalability
- Able to exploit the computer's physical threads.



Comparison with other implementations



Conclusion



Alternative processes

Shake processes

Post-ionization, the different number of particles in the system leads to a change in the Hamiltonian. This leads to the lack of orthogonality between non-equivalent states and free-wave wavefunctions in the initial and final configurations.

$$\langle 1s_i | 2s_f \rangle \neq 0 \quad \langle 1s_i | e_{\text{free}}^- \rangle \neq 0$$

Shake-up

Excitation of extra electron(s).

Shake-off

Ionization of extra electron(s).

Alternative processes

Shake processes

Post-ionization, the different number of particles in the system leads to a change in the Hamiltonian. This leads to the lack of orthogonality between non-equivalent states and free-wave wavefunctions in the initial and final configurations.

$$\langle 1s_i | 2s_f \rangle \neq 0 \quad \langle 1s_i | e_{\text{free}}^- \rangle \neq 0$$

Shake-up

Excitation of extra electron(s).


Shake-off

Ionization of extra electron(s).

Alternative processes

Shake processes

Post-ionization, the different number of particles in the system leads to a change in the Hamiltonian. This leads to the lack of orthogonality between non-equivalent states and free-wave wavefunctions in the initial and final configurations.



$$\langle 1s_i | 2s_f \rangle \neq 0 \quad \langle 1s_i | e_{\text{free}}^- \rangle \neq 0$$

Shake-up

Excitation of extra electron(s).

Shake-off

Ionization of extra electron(s).

Alternative processes

Shake Processes

The probability of these processes occurring is extremely dependent on the incident energy.

Since for this thesis, the energy ranges studied were below the ionization threshold, no shake processes were accounted for.

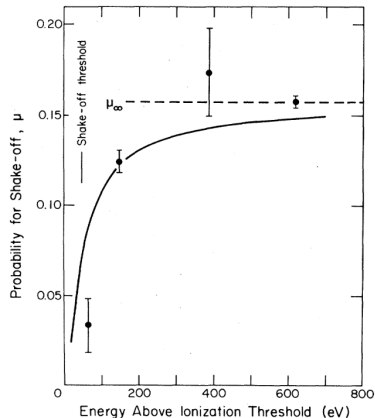


Figure: Thomas model for shake probability. [1]

Radiative transitions

Given the set of all 1-hole levels, with n elements, the total number of these transitions (without accounting for level degeneracy), N , is simply given by the amount of combinations of two elements between the set:

$$N = \frac{n!}{2 \cdot (n-2)!}$$

For these transitions, **full orbital relaxation** was allowed.

The *mcdfgme* calculation yields the rates for each Electric and/or Magnetic component/pole for both Coulomb (length) and Lorentz (velocity) gauges.

Auger transitions

The total number of Auger transitions can not be calculated *a priori*. Since the 1-hole and 2-holes level sets are "independent", the level structure needs to be calculated in order to fully resolve the number of transitions. For computing these transitions, the free-electron wavefunction has to be computed for the initial state potential, and **orthogonality is enforced** between the free-wave and bound orbitals.

The theoretical spectral shape

Based on all previously computed atomic parameters, it is now possible to start simulating spectral lines.

The theoretical spectral shape

Lorentzian profile

Describes the theoretical line shape for the emission:

$$\frac{I_{i,f}}{2\pi} \frac{\Gamma_{i,f}}{(E - E_{i,f})^2 + (\Gamma_{i,f}/2)^2}$$

Does not account for **thermal distributions** and **stochastic events**.

The theoretical spectral shape

Lorentzian profile

Describes the theoretical line shape for the emission:

$$\frac{I_{i,f}}{2\pi} \frac{\Gamma_{i,f}}{(E - E_{i,f})^2 + (\Gamma_{i,f}/2)^2}$$

Does not account for **thermal distributions** and **stochastic events**.

Gaussian profile

This profile will be used to account for any **broadening effects** that may impact the measured spectra.

$$\frac{1}{\sigma\sqrt{2\pi}} \exp\left(-\frac{E^2}{2\sigma^2}\right)$$

The theoretical spectral shape

Lorentzian profile

Describes the theoretical line shape for the emission:

$$\frac{I_{i,f}}{2\pi} \frac{\Gamma_{i,f}}{(E - E_{i,f})^2 + (\Gamma_{i,f}/2)^2}$$

Does not account for **thermal distributions** and **stochastic events**.

Gaussian profile

This profile will be used to account for any **broadening effects** that may impact the measured spectra.

$$\frac{1}{\sigma\sqrt{2\pi}} \exp\left(-\frac{E^2}{2\sigma^2}\right)$$

The convolution of both gives rise to the **Voigt profile**, incorporating all the desired effects, at the cost of computational power.

The theoretical spectral shape

